INTERNATIONAL JOURNAL OF CHEMICAL REACTOR ENGINEERING

Volume 6 2008 *Article* A19

Conceptual Analysis of a Cyclic Water Gas Shift Reactor

Peter Heidebrecht* Christoph Hertel†

Kai Sundmacher‡

*Max-Planck-Institute for Dynamics of Complex Technical Systems, heidebrecht@mpi-magdeburg.mpg.de

†Max-Planck-Institute for Dynamics of Complex Technical Systems, hertel@mpi-magdeburg.mpg.de

‡Max-Planck-Institute for Dynamics of Complex Technical Systems & Otto-von-Guericke University, sundmacher@mpi-magdeburg.mpg.de

ISSN 1542-6580

Conceptual Analysis of a Cyclic Water Gas Shift Reactor

Peter Heidebrecht, Christoph Hertel, and Kai Sundmacher

Abstract

The cyclic water gas shift reactor (CWGSR) is based on the repeated reduction of a fixed bed using a mixture of hydrogen and carbon monoxide and its subsequent oxidation with steam to produce pure hydrogen. The reactor is analyzed on a conceptual level using a spatially distributed, dynamic model. The model assumptions and the resulting model equations are presented, and important parameters are discussed. Simulation results show that the CWGSR reactor has a poor performance for co-flow configuration of the gases during reduction and oxidation phase, but the reverse-flow configuration seems to be a very attractive option. Parameter variation of the duration of the reduction phase indicates that especially short cycling times not only yield high energetic performance, but they also decrease thermal and morphological stress on the fixed bed material. In addition, the counter-flow CWGSR with short cycling times shows an inherent heat integration like in a Matros reactor, which opens attractive options for system integration of this reactor with other process steps. The behavior of the CWGSR is compared to a pressure swing adsorption reactor (PSA), which shows common features, but also significant differences between both types of cyclic fixed bed reactors.

KEYWORDS: cyclic operation, fixed bed reactor, water gas shift reaction, mathematical model

1. Introduction

A number of actual and future applications require carbon monoxide free hydrogen. Carbon monoxide is a strong catalyst poison, especially for noble catalysts, limiting its tolerable concentration in low temperature fuel cells like the PEMFC (Polymer electrolyte membrane fuel cells, using Platinum electrodes) to 10 ppm. The production of hydrogen was and is still mainly based on fossil fuels like gas, oil and coal and – to a small, but steadily increasing part – from biomass. Apart from the energy intensive Kvaerner process (Lynum et al, 1999), which is restricted to gaseous educts, gasification and reformation processes are applied which usually deliver a mixture of hydrogen, carbon monoxide and carbon dioxide. The cleaning of these gas mixtures from carbon monoxide is usually done via the water gas shift reaction:

$$CO + H_2O \rightarrow CO_2 + H_2$$

Depending on the desired purity level, this process usually comprises several steps like high and low temperature shift reactors, pressure swing adsorption or others. This often leads to a considerable effort for the cleaning process with energetic losses and high investment costs. A simplification of the cleaning process in one single reactor could provide a breakthrough for many energetic and chemical applications. The cyclic water gas shift reactor (CWGSR) could be a solution to this problem.

The water gas shift reaction is a redox reaction, where the carbon within the carbon monoxide is oxidized and the hydrogen within the water molecules is reduced. The principle of the CWGSR is the temporal separation of the two parts of this redox reaction. This is achieved with the help of a fixed bed of some metal oxide, preferably iron oxide (Figure 1). At first, a gas mixture containing carbon monoxide – and possibly hydrogen, if the gas originates from a reforming reactor – is fed into the reactor, reducing the iron oxide. During this, carbon dioxide and water are produced:

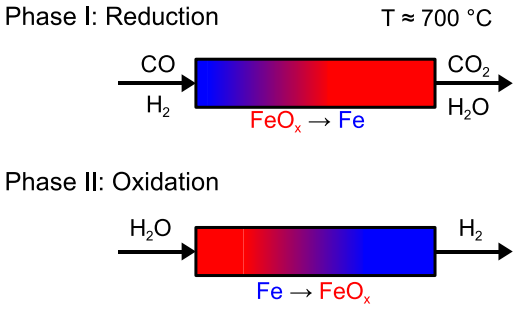

Figure 1. Principle of the cyclic water gas shift reactor (CWGSR).

$$CO + 1/x\ FeO_x \rightarrow CO_2 + 1/x\ Fe$$

$$H_2 + 1/x\ FeO_x \rightarrow H_2O + 1/x\ Fe$$

After a while, when the bed is reduced to a sufficient extent, the feed is switched to steam, which then oxidizes the iron to iron oxide, producing pure hydrogen without contaminants like carbon monoxide at the outlet of the reactor:

$$H_2O + 1/x\ Fe \rightarrow H_2 + 1/x\ FeO_x$$

The CWGSR, which is sometimes referred to as sponge iron process, can be compared to other cyclic processes such as a conventional fixed bed reactor or a pressure swing adsorption process. In a fixed bed reactor (e.g. Glöckler et al., 2003; Kulkarni and Dudukovic, 1998), the gas flows through porous solid material, which acts as catalyst and as heat storage. Usually, the heat capacity of the fixed bed is much larger than that of the gas inside the reactor, so in addition to the gas composition, which can change very quickly in a fixed bed reactor, the reactor temperature is the important state variable, dominated by a large time constant. In the CWGSR, the fixed bed also serves as an oxygen storage. The degree of reduction, which describes the oxygen content of the fixed bed, determines the reaction rates in the reactor and is thus the second important state variable. As with the heat storage, the oxygen capacity of the fixed bed is significantly higher than the capacity of the gas, so this state variable is also dominated by a large time constant.

Another process similar to the CWGSR is the pressure swing adsorption (PSA, e.g. Malek and Farooq, 1998; Sircar and Golden, 2000). In addition to temperature, which can play an important role in this process, the coverage of the adsorbed species is a second, slow state variable, influencing the adsorption kinetics. Pressure is an important state in PSA, but it is governed by a very low time constant and is not related to the fixed bed. Although the fixed bed in PSA has two state variables (temperature and coverage), it is still different from the CWGSR. In PSA, one or more gas components are adsorbed from the gas stream and the phase is ended before the bed is saturated with these components and they eventually break through. In the desorption phase the focus is to desorb the components again by an auxiliary gas stream. The quality of the output gases during this phase or the phase duration is only of secondary importance. In the CWGSR, the desorption phase corresponds to the reduction phase, where the valuable fuel gas is consumed to reduce the fixed bed. Gas utilization and phase duration are highly important during this phase.

With this in mind, it is evident that although the CWGSR shares some aspects with conventional fixed bed or pressure swing adsorption processes, it has its own unique characteristics which need to be understood for a thorough process design. Although the process idea is not new (Messerschmitt, 1911; Hacker et al., 1998; Hacker et al., 2000), the system has not yet been analyzed on a conceptual level. The aim of this analysis is to give some understanding of the basic behavior of this reactor and to draw some relevant conclusions for the reactor design rather than going into the details of reaction kinetics, mass and heat transfer. Therefore,

a model is set up which neglects a number of aspects like thermodynamic equilibria and complex kinetics in order to capture the very basic behavior of the CWGSR. This model is then used to evaluate suitable operating modes and conditions.

2. Dimensionless model

For a conceptual analysis of the CWGSR a transient, spatially one-dimensional model is sufficient. Simplifying assumptions are set up (see section 2.1) to describe representative gas phase concentrations, flow rates and temperatures (section 2.2). All model equations are then expressed in terms of dimensionless parameters, so a very general description is obtained which can be applied to a CWGSR of any size (section 2.3). The values of the most important model parameters are given at the end of this chapter (section 2.4).

2.1 Model assumptions

The model is derived under the following assumptions:

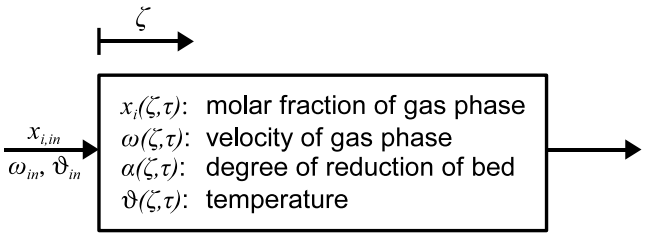

Figure 2. Scheme of the model of the CWGSR. States at the gas inlet and inside the reactor are indicated.

- The reactor has a constant cross sectional area. Its length is much higher than its width. The two phases (gas phase and solid fixed bed material) occupy constant volume fractions within the reactor. Heat exchange with the environment across the reactor walls is considered by a linear approach.
- The gas is assumed to be ideal. Friction forces and gravity are neglected. Isobaric conditions are applied. Due to the fixed bed, plug flow is assumed. Due to high gas velocities, axial diffusion and heat conduction in the gas phase are neglected.
- The fixed bed material consists of two components: reduced and oxidized species. The relative amount of these is described by the degree of reduction. Changes of the properties of the fixed bed material due to reduction or oxidation are neglected. A constant axial heat conductivity is assumed.
- The reduction and oxidation reactions are of 1st order with respect to the gas concentrations and the degree of reduction of the fixed bed. Mass transport is not explicitly considered.
- The kinetics of heat exchange between solid and gas are very fast, so a pseudo homogeneous enthalpy balance for both phases is used.

2.2 Dimensional equations

Given the assumptions listed above, one can derive a spatially one-dimensional model. In the gas phase, two states are of interest: the gas velocity and the gas compositions, described here in terms of molar fractions. The gas compositions are given by the following transient partial differential equation:

$$c_t \varepsilon \cdot \frac{\partial x_i}{\partial t} = -c_t \varepsilon \cdot v \cdot \frac{\partial x_i}{\partial z} + (1-\varepsilon) \cdot a \cdot \sum_j \left(\nu_{i,j} - x_i \bar{\nu}_j \right) \cdot r_j \tag{1}$$

With the accumulation term on the left hand side of the equation, the first term on the right hand side can be identified as the convective term along the reactor axis. The last term considers the change in concentrations due to reaction and due to non-equimolar reactions (which do not occur in this specific example). The total gas concentration is computed according to the ideal gas law. This equation requires an initial condition for the molar fractions and a boundary condition, which is given by the gas composition at the gas inlet of the reactor (Figure 2).

The total mass balance in combination with the ideal gas law and the isobaric assumption yields the following equation which can be used to calculate the gas velocity:

$$0 = -\frac{\partial v}{\partial z} + \frac{1-\varepsilon}{\varepsilon} \cdot \frac{a}{c_t} \cdot \sum_j \bar{\nu}_j \cdot r_j + \frac{1}{T} \cdot \frac{\partial T}{\partial t} + \frac{v}{T} \cdot \frac{\partial T}{\partial z} \tag{2}$$

The second term considers the effect of non-equimolar reactions on the gas velocity, while the last two terms account for temperature effects, for example gas expansion due to increasing temperature. The only boundary condition required to solve this equation is given by the gas velocity at the reactor inlet.

In addition to the gas phase equations, the fixed bed needs to be described. The following ordinary differential equation is a molar mass balance of the reduced metal species and takes into account the reduction and oxidation reactions:

$$\frac{\partial c_{Fe}^a}{\partial t} = \sum_j \nu_{Fe,j} r_j \tag{3}$$

Only an initial condition for the concentration of the reduced species is required.

The pseudo-homogeneous enthalpy balance assumes that the temperatures of both gas and solid are identical:

$$(1-\varepsilon)\,c_p^S\cdot\frac{\partial T}{\partial t}=-\varepsilon\,v\,c_p^G\cdot\frac{\partial T}{\partial z}+(1-\varepsilon)\,\lambda\cdot\frac{\partial^2 T}{\partial z^2} +(1-\varepsilon)a\cdot\sum_j(-\Delta_R h_j^\theta)\,r_j+\frac{2}{R_r}k^h\cdot(T_e-T) \tag{4}$$

The accumulation term contains the heat capacity of the fixed bed material, whereas the capacity of the gas phase is neglected. The convection term only considers heat transport in the gas phase, while the second derivative describes the heat conduction in the fixed bed material according to Fourier's law. The third term accounts for the heats of reaction and the last term stands for the heat exchange with the environment across the reactor walls. This equation requires the reactor temperature profile as initial condition. The two required boundary conditions are given by the gas temperature at the reactor inlet and a zero temperature gradient at the opposite end of the reactor.

2.3 Dimensionless equations

With the dimensional equations listed above and the definitions of the dimensionless parameters (see notation table), the following set of equations forms the dimensionless model equations:

$$\frac{\partial x_i}{\partial\tau}=-\omega\frac{\partial x_i}{\partial\zeta}+\vartheta\cdot\sum_j\left(\nu_{i,j}-x_i\bar{\nu}_j\right)\cdot Da_j\cdot R_j \tag{5}$$

$$0=-\frac{\partial\omega}{\partial\zeta}+\vartheta\cdot\sum_j\bar{\nu}_j\cdot Da_j\cdot R_j+\frac{1}{\vartheta}\cdot\frac{\partial\vartheta}{\partial\tau}+\frac{\omega}{\vartheta}\cdot\frac{\partial\vartheta}{\partial\zeta} \tag{6}$$

$$\Theta\cdot\frac{\partial\alpha}{\partial\tau}=\sum_j\nu_{Fe,j}\,Da_j\,R_j \tag{7}$$

$$\Psi\cdot\frac{\partial\vartheta}{\partial\tau}=-\omega\cdot\frac{\partial\vartheta}{\partial\zeta}+\frac{1}{Pe}\cdot\frac{\partial^2\vartheta}{\partial\zeta^2}+\Psi\cdot\sum_j\Delta\vartheta_{ad,j}\cdot Da_j R_j-St\cdot\left(\vartheta-\vartheta_e\right) \tag{8}$$

Note that the dimensionless temperature occurs as a factor in Eqs. 5 and 6, where it replaces the reciprocal total gas concentration, c_t. The temperature, ϑ, is the dimensional temperature divided by a typical CWGSR temperature. The gas velocity, ω, is the dimensional velocity related to a typical gas velocity at the reactor inlet. With this definition, both variables are in the order of magnitude of 1.

Reaction rates are required for the reactions of carbon monoxide to carbon dioxide and of hydrogen to water. They include an Arrhenius term to account for

the temperature dependence of the reaction rates. The kinetics usually are assumed to be of first order with respect to each gas concentration, but this reaction order can be varied. The following reactions are considered:

r_1: $H_2O + Fe \rightarrow H_2 + FeO_x$

r_2: $H_2 + FeO_x \rightarrow H_2O + Fe$

r_3: $CO_2 + Fe \rightarrow CO + FeO_x$

r_4: $CO + FeO_x \rightarrow CO_2 + Fe$

$$R_1 = \exp\left(\gamma_1 \cdot \left(1 - \frac{1}{\vartheta}\right)\right) \cdot x_{H_2O}^{n_1} \cdot \alpha \tag{9}$$

$$R_2 = \exp\left(\gamma_2 \cdot \left(1 - \frac{1}{\vartheta}\right)\right) \cdot x_{H_2}^{n_2} \cdot (1-\alpha) \tag{10}$$

$$R_3 = \exp\left(\gamma_3 \cdot \left(1 - \frac{1}{\vartheta}\right)\right) \cdot x_{CO_2}^{n_3} \cdot \alpha \tag{11}$$

$$R_4 = \exp\left(\gamma_4 \cdot \left(1 - \frac{1}{\vartheta}\right)\right) \cdot x_{CO}^{n_4} \cdot (1-\alpha) \tag{12}$$

The ratios Da_1/Da_2 and Da_3/Da_4 can be interpreted as some kind of equilibrium constants, although this is not strictly applicable in gas-solid reactions.

2.4 Model parameters

Among the most important parameters in this model are the reaction specific Damköhler numbers, *Da*. Their magnitude is a measure for the reactor size relative to the inlet gas flow. The ratio between two Damköhler numbers is the relative activity of the fixed bed material with respect to the two reactions. As the size of the reactor is not yet fixed, the Damköhler numbers can be chosen arbitrarily for each simulation. However, preliminary experiments conducted with a differential reactor with a fixed bed material based on Fe_2O_3-CeO_2 (Figures 3a and 3b, from Galvita and Sundmacher, 2007) indicate that the reduction with H_2 (reaction 2, Figure 3a) is about 3 to 5 times slower than the oxidation using H_2O (reaction 1, Figure 3b). This fact should be reflected by the ratio of the Damköhler numbers Da_1 and Da_2.

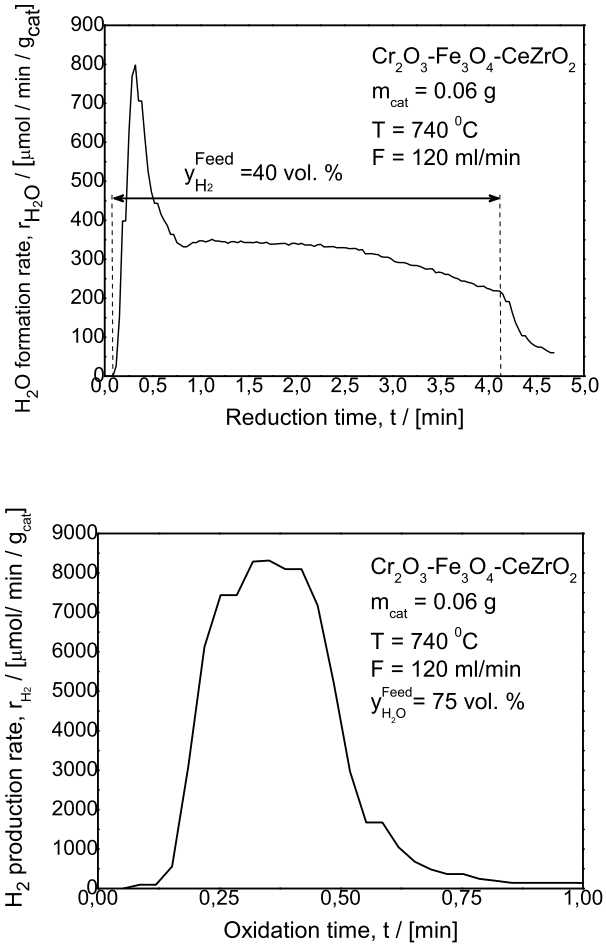

Figure 3. Experimental data from a reduction (top) and oxidation (bottom) of a small sample of Fe_2O_3-CeO_2 with H_2 and H_2O, respectively. The reduction is about 3 times slower than the oxidation. From Galvita and Sundmacher, 2007.

Concerning the values of the Damköhler numbers, the breakthrough behavior of the reactor is essential. Ideally, a breakthrough of contaminated hydrogen during the reduction phase should only occur after the complete fixed bed has been fully reduced. At that time, the feed streams would be switched and the oxidation phase would begin. Only for Damköhler numbers approaching infinity the CWGSR would show such behavior. For very low Damköhler numbers, only a small portion of the contaminated hydrogen would be utilized to reduce the fixed bed, the rest of the gas would be lost for the process. Thus, high Damköhler numbers are preferred. In the simulations in this work, we generally apply Da_1=50 and Da_2=15, which takes into account the ratio between both reaction rates and which is a compromise between ideal reactor behavior and limited reactor size.

Besides the Damköhler numbers, four important parameters can be identified, two of them are capacities. The substantial fixed bed capacity, Θ, is the ratio between the oxygen capacity of the fixed bed and the gas hold up of the reactor. Due to the low density of gas under ambient pressure and at high temperature, and due to the high oxygen capacity of the fixed bed material, this ratio is at about 10^3. The thermal capacity, Ψ, relates the heat capacity of the fixed bed to the heat capacity of the gas phase, and is at about 10^4. This means that Equations (7) and (8) are governed by large time constants and change fairly slowly compared to the gas composition, which has a time constant of 1.

Further parameters are the dimensionless heats of reaction, $\Delta\vartheta_{ad,j}$, which are the negative reaction enthalpy divided by the heat capacity of the gas phase and the standard temperature. For the oxidation of H_2 (reaction 2), this is $-6\cdot10^{-5}$, while for the oxidation of CO (reaction 4) its value is $4\cdot10^{-5}$. The heats of reaction 1 and 3 have the same absolute values, but different signs ($+6\cdot10^{-5}$ and $-4\cdot10^{-5}$). Although these values seem negligible, note that they are always multiplied with the dimensionless heat capacity, Ψ, which is rather large. To consider the temperature effect on the reaction rate, Arrhenius numbers, γ_j, are introduced. They are defined as activation energies divided by the gas constant and the standard temperature. With a standard temperature of 1000 K and an estimated activation energy of 70 kJ/mol, the Arrhenius numbers are at about 8.4. The Arrhenius numbers are assumed to be identical for all reactions, as kinetic experiments are currently being conducted and no reliable values are available in the literature for the considered reactions.

3. Isothermal simulations

In the simulations of this chapter, Equation (8) is not used, but isothermal conditions (ϑ=const.) are applied. In addition, carbon monoxide is not explicitly considered here during the reduction phase. The only effect of considering carbon monoxide would be that the whole reaction would be exothermic, which is irrelevant in case of an isothermal model. Nevertheless, the hydrogen which is fed into the reactor during the oxidation phase is considered contaminated. The inlet velocities are always $\omega_{in}=\pm1$, depending on the flow direction.

The duration of the reduction phase can be fixed arbitrarily. In the simulations shown, this duration was chosen long enough to reduce a major part of the fixed bed, which was the case with $\tau_{reduction} = 2000$. The duration of the oxidation phase was determined using a quality specification of the hydrogen product. As soon as the hydrogen concentration in the product stream dropped below 90 mol-%, the oxidation phase was stopped and the reduction phase was initiated.

The simulation results show the cyclic steady state, i.e. the repeating cycle which the system attains after a sufficient number of cycles. Starting with arbitrarily chosen initial conditions (no reactants inside the channel, fully oxidized fixed

bed), only three to five cycles were necessary to bring the isothermal simulations with long cycle durations into a cyclic steady state.

3.1 Co-flow operation

At the beginning of the oxidation phase, the fixed bed is virtually completely reduced and steam is fed into the reactor on the left hand side. Most of the steam is converted to hydrogen. Due to the high Damköhler number of the dominant reaction, Da_1, the reaction proceeds in a front-like shape along the reactor (Figure 4). With time, this front moves along the reactor and eventually reaches its right end. When this happens, the hydrogen concentration in the output stream decreases below the given limit and the reduction phase is initiated.

At the end of the oxidation phase, most of the fixed bed is completely oxidized, but a considerable amount near the right hand side of the reactor is still in a reduced state (see the red curves in Figure 4, right). With this fixed bed, the reduction phase is initiated by feeding contaminated hydrogen into the left end (Figure 5, left). This hydrogen is converted to steam, whereby the reduction degree of the fixed bed is rising near the inlet. Towards the reactor's end, the produced steam meets the reduced fixed bed, so oxidation occurs near the reactor outlet (see both Figures 5). Due to this, the reactor produces contaminated hydrogen, which must be considered as lost fuel gas for the process.

To avoid the losses at the reactor's rear end, the fixed bed there must be oxidized. This can be realized by extending the oxidation phase duration. In that case, the hydrogen concentration at the output would decrease quickly and approach zero. The changing hydrogen concentration may pose a problem for the following processes, but even if not, extending the oxidation phase brings losses in steam and costs time, reducing the efficiency of the process and its production capacity per time.

If not during an extended oxidation phase, the fixed bed near the reactor outlet is reduced after sufficient time during the reduction phase. However, the oxidation occurring during the reduction phase is a clear sign of inefficiency. This can also be seen figuratively in the profiles of the reduction degree at the beginning of each phase. While $\alpha(\zeta)$ increases along the reactor coordinate at the end of the oxidation phase (Figure 4, right), it has a falling slope at the end of the reduction phase (Figure 5, right). The necessary inversion of this profile during each phase can be interpreted as the reason for losses in the feed gas.

Furthermore, notice that the reduction does not proceed in a sharp front, but the concentration profiles show a distinct slope. This is due to the lower Damköhler number of the prevailing reaction, Da_2. Thus a considerable amount of contaminated feed gas is lost in order to obtain a high degree of reduction throughout the reactor.

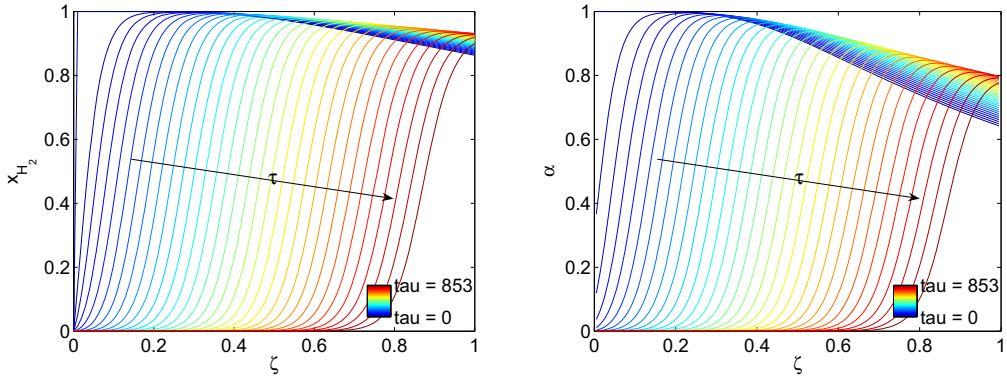

Figure 4. Molar fraction of hydrogen (reaction product, left) and degree of reduction (right) in a co-flow CWGSR during the oxidation phase. Hydrogen is produced in a moving front and the fixed bed material is oxidized from left to right.

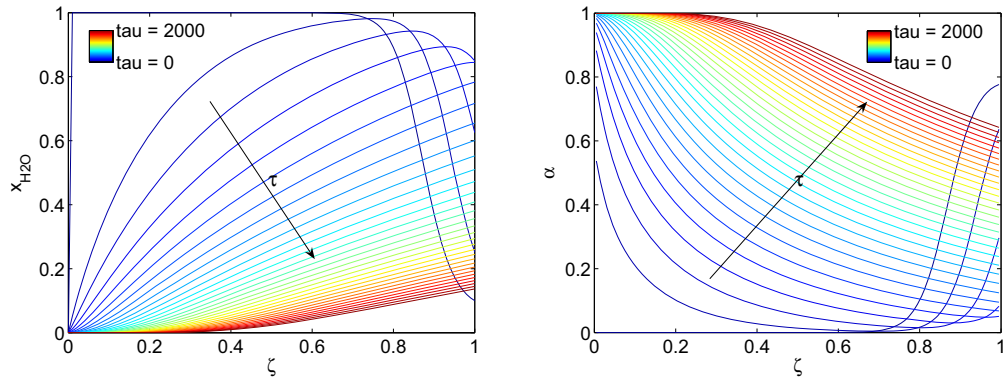

Figure 5. Molar fraction of water (reaction product, left) and degree of reduction (right) in a co-flow CWGSR during reduction phase. In the beginning (τ=0) in the rear end (ζ=1), water is consumed and the bed is oxidized. The hydrogen produced therein can not be used and is lost.

Gas losses are also known from pressure swing adsorption reactors (PSA). However, there are certain differences between the CWGSR and PSA. Considering a PSA for the removal of CO from a reformate gas, the adsorption phase in the PSA is comparable to the oxidation phase in the CWGSR, and the free adsorption surface is the analogue of the degree of reduction. The duration of the adsorption and oxidation phase are both determined by the exhaustion of the fixed bed. In the PSA desorption phase, a sweep gas is used to clean the fixed bed under reduced pressure. Inefficiencies due to co-flow configuration cost additional time and sweep gas, which is an auxiliary component. In the case of CWGSR, this causes losses in valuable fuel gas. This difference has its impact on the operation of a CWGSR.

3.2 Reverse-flow operation

The drawbacks of the co-flow CWGSR are amended under reverse-flow operation, that is if the gas flow direction is reversed during the oxidation phase. Figure 6 shows the profiles of the steam concentration and the degree of reduction during the reduction phase, which are monotonous throughout the whole phase. The advantage of reverse-flow operation is also emphasized in Figure 7, where the outlet concentrations are shown for both modes of operation. The red dashed line shows again that after the reduction phase has begun, a considerable amount of hydrogen leaves the reactor due to the non-oxidized end of the fixed bed. In opposite to that, the profile for reverse-flow not only shows a favorably high hydrogen concentration during the oxidation phase, but it also has a fast transition at the switching time from oxidation to reduction phase. These two aspects make the reverse-flow operation superior to co-flow operation mode.

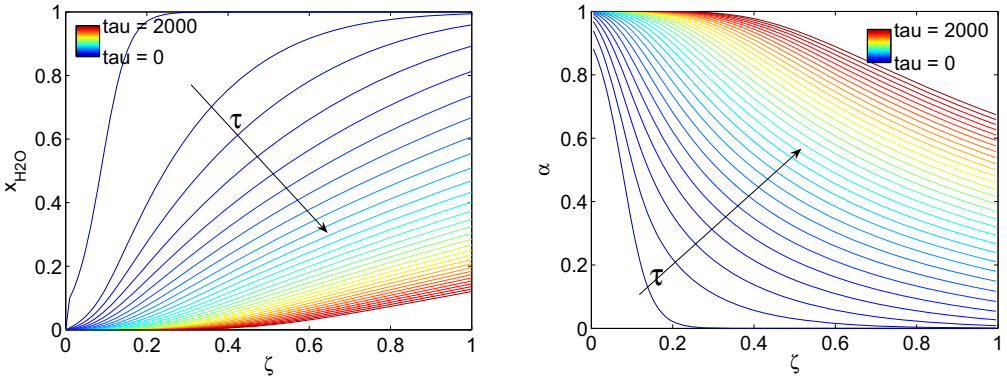

Figure 6. Molar fraction of water (reaction product, left) and degree of reduction (right) in a reverse-flow CWGSR during the reduction phase.

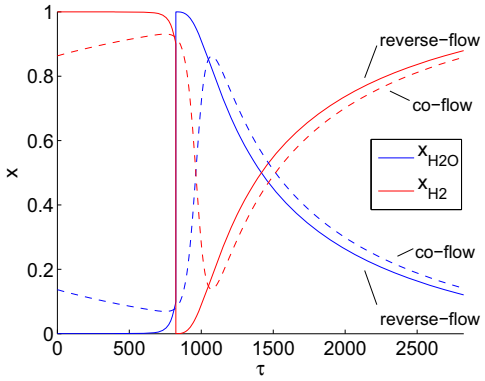

Figure 7. Output concentrations in co-flow (dashed lines) and reverse-flow (full lines) operation modes. The reverse-flow configuration produces higher concentration of hydrogen and shows less losses of combustible gases.

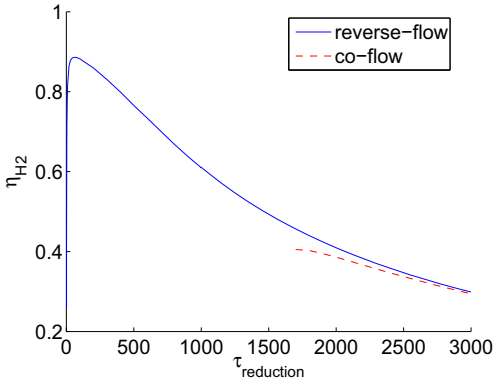

Figure 8. Energetic efficiencies for co- and reverse-flow operation as a function of the duration of the reduction phase.

These qualitative findings are not depending on the chosen reaction kinetics. Although the actual curves look different, other orders of reactions with respect to the gas phase and to the degree of reduction show the same basic behavior for co-flow and reverse-flow. Thus the reverse-flow is preferable over co-flow independent of the real kinetics in the CWGSR.

3.3 Efficiency and cycling duration

The CWGSR is meant to be used in electric power plants based on fuel cells. Therefore, one of the most important issues is the efficiency of the CWGSR. Defining the efficiency as the total amount of clean hydrogen obtained during the oxidation phase divided by the amount of contaminated hydrogen fed into the reactor during the reduction phase yields the following expression:

$$\eta_{H_2} = \frac{\int_{oxidation} \left(\omega / \vartheta \cdot x_{H_2}\right)_{out} d\tau}{\int_{reduction} \left(\omega / \vartheta \cdot x_{H_2}\right)_{in} d\tau} \tag{5}$$

For a given set of parameters, the reduction phase duration can be varied in order to increase the efficiency of the CWGSR. As before, the oxidation phase is stopped as soon as the molar fraction of hydrogen in the output gas drops below 0.9. The result of this parameter study is shown in Figure 8. In the case of co-flow configuration, the reduction phase has to last at least 1700 dimensionless time units, otherwise a hydrogen output concentration of 90 % can not be obtained. In reverse-flow operation, cycling times can be decreased considerably, with the resulting efficiency increasing steadily up to 90%. However, the maximum is not obtained at infinitely short cycle duration, but at about $\tau_{reduction}$=70. This is because after the switching of gas streams, the first portion of outlet gases must be considered contaminated and can not be used as product gas, which is accounted for in the calculation. Thus, the reverse-flow operation mode with short cycle durations seems to be favorable and promises high energetic efficiencies.

The short cycle duration has an additional advantage over long cycle times. As seen in Figures 4 to 6, long cycle times lead to repeated large changes in the degree of reduction over time. This leads to strong morphological changes of the fixed bed material. The consequence is fast sintering and thereby the deactivation of the metal oxide. Applying short cycle durations means that the reduction degree of the fixed bed does not change much anywhere in the reactor, as can be seen in Figure 9 ($\tau_{reduction}$=70). This reduces the stress of the material and significantly delays its deactivation.

The fact that short cycle durations are preferred is what discriminates the CWGSR from a pressure swing adsorption reactor. In a PSA, the adsorption phase lasts until short before a breakthrough. After depressurization, these species are

desorbed again until the bed is nearly completely free. Although this is a simplified description of real PSA processes, the point is that the adsorption bed is nearly completely filled and emptied again, which corresponds to long cycle durations. Applying short cycle times to the CWGSR means that a partially loaded fixed bed is loaded with a small additional amount of oxygen and then unloaded again by the same amount. Deep reduction or oxidation are thus avoided in the CWGSR.

4. Non-isothermal simulations

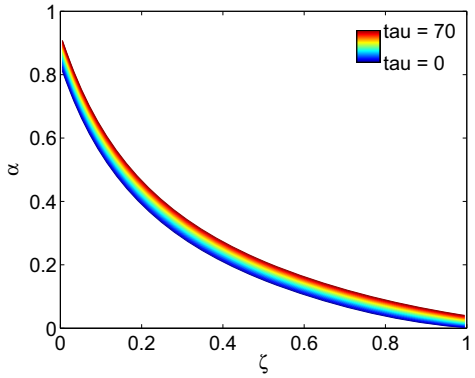

Figure 9. Degree of reduction during reverse-flow operation with short phase duration. The small changes help reduce material deactivation.

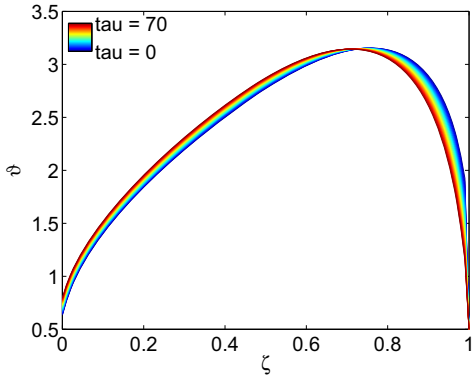

Figure 8. Temperature during reverse-flow operation with short phase duration and similar phase durations for oxidation and reduction. The CWGSR works as a Matros reactor.

After a suitable operating regime for the CWGSR is identified, the thermal behavior is simulated. This is done using the full model (Equations (5) to (8)) including the enthalpy balance. Starting from arbitrary initial conditions, the slow fixed bed states do not change much during each short cycle, so it usually takes several thousand cycles to obtain a cyclic steady state. In this simulation, a mixture of hydrogen and carbon monoxide is fed into the reactor during the reduction phase, so the net reaction is exothermic. Due to the short cycling times, the temperature profile does not change much during each cycle, which is also favorable with respect to thermally controlled deactivation mechanisms. Applying nearly similar durations for the reduction and for the oxidation phase as well as a low inlet temperature of ϑ_{in}=0.5 leads to an interesting thermal behavior. The net heat released by the water gas shift reaction inside the reactor is convectively transported by the gas flows. In reverse-flow operation, the direction of this transportation mechanism changes frequently, so that for short cycle times, the heat is captured inside the reactor (see Figure 8). This behavior is known from so-called Matros reactors (Matros et al., 1989; Matros et al, 1993) and can be utilized to integrate the

CWGSR into a system without extensive heat exchangers at the inlet and outlet. Relatively cool gas can be supplied into the reactor, which can sustain a high temperature level and emit relatively cold product gases.

5. Conclusions and outlook

The cyclic water gas shift reactor is a fixed bed reactor for the production of carbon monoxide free hydrogen. Although it has some common aspects with a cyclically operated catalytic fixed bed reactor or a pressure swing adsorption reactor, it has some unique features that are analyzed and discussed on a conceptual level in this contribution.

The simulation of the cyclic behavior shows that the co-flow mode of operation has certain drawbacks that curtail its efficiency and lead to high deactivation rates of the fixed bed material. Instead, we suggest to apply a reverse-flow operation mode. Although reverse-flow is more difficult to realize practically, it has significant advantages. Fuel losses occurring in co-flow mode are avoided here and the slope of the reduction profile does not change its sign during each cycle phase. Applying short cycle times can further improve the performance of the reverse-flow mode. Efficiency can reach up to 90% and the almost constant reduction degree of the fixed bed slows down deactivation processes. In addition, a reverse-flow reactor with short cycle duration can work in a heat-integrated manner like a Matros reactor, which offers attractive options for system integration with other process steps like a steam reformer or a low temperature fuel cell.

Further works on the CWGSR include a more detailed modeling of the reactor, taking into account multiple reaction steps, non-linear reaction kinetics (Avrami-Erofeev or diffusion limited kinetics) and radial distributions in the gas flow and temperature. Simultaneously, kinetic experiments are being conducted that will help to understand and incorporate the microscopic behavior of the fixed bed material, and a lab scale CWGSR is being constructed to validate the simulation results from the advanced models.

Notation

In case of dimensional parameters, their unit is given. For dimensionless parameters their definition in terms of dimensional parameters is given.

Latin symbols

a	$[m^2 \cdot m^{-3}]$	Fixed bed surface area per reactor volume
c_{Fe}^{a}	$[mol \cdot m^{-2}]$	Surface related iron concentration
c_p	$[J \cdot m^{-3} \cdot K^{-1}]$	Volume related heat capacity
c_t	$[mol \cdot m^{-3}]$	Total molar concentration gas phase

$Da_j = \frac{(1-\varepsilon) a L r_j^\theta}{\varepsilon v^\theta c_t^\theta}$	$[-]$	Damköhler number (reaction rate constant) of reaction j
$E_{a,j}$	$[J \cdot mol^{-1}]$	Activation energy reaction j
k^h	$[W \cdot m^{-2} \cdot K^{-1}]$	Heat transfer coefficient across reactor walls
L	$[m]$	Reactor length
n_j	$[-]$	Order of reaction j
$Pe = \frac{\varepsilon v^\theta c_{p,g}}{(1-\varepsilon)\lambda / L}$	$[-]$	Peclet number (inverse heat conductivity) of the fixed bed
R	$[J \cdot mol^{-1} \cdot K^{-1}]$	Gas constant
$R_j = \frac{r_j}{r_j^\theta}$	$[-]$	Reaction rate of reaction j
R_r	$[m]$	Reactor radius
r_j	$[mol \cdot m^{-2} \cdot s^{-1}]$	Surface related reaction rate of reaction j
$St = \frac{2L / v^\theta k^h}{R_r \varepsilon c_{p,g}}$	$[-]$	Stanton number (heat exchange coef.) with the environment
T	$[K]$	Temperature
t	$[s]$	Time
v	$[m \cdot s^{-1}]$	True gas velocity
x_i	$[-]$	Molar fraction of component i
z	$[m]$	Spatial coordinate

Greek symbols

$\alpha = \frac{c_{Fe}^a}{c_{Fe,max}^a}$	$[-]$	Degree of reduction of the fixed bed
$\gamma_j = \frac{E_{A,j}}{RT^\theta}$	$[-]$	Arrhenius number (activation energy) of reaction j
$\Delta \vartheta_{ad,j} = \frac{-\Delta_R h_j^\theta \varepsilon c_t^\theta}{(1-\varepsilon) c_{p,s} T^\theta}$	$[-]$	Adiabatic temperature increase due to reaction j
$\Delta_r h_j^\theta$	$[J \cdot mol^{-1}]$	Reaction enthalpy of reaction j
ε	$[-]$	Fixed bed porosity, gas volume fraction
$\zeta = \frac{z}{L}$	$[-]$	Axial reactor coordinate
η	$[-]$	Energetic efficiency
$\Theta = \frac{(1-\varepsilon) a c_{Fe,max}^a}{\varepsilon c_t^\theta}$	$[-]$	Substantial (oxygen) capacity of the fixed bed

$\vartheta = \frac{T}{T^{\theta}}$	[-]	Reactor temperature
λ	$[W \cdot m^{-1} \cdot K^{-1}]$	Heat conductivity fixed bed material
$\nu_{i,j}$	[-]	Stoichiometric coefficient of gas component i in reaction j
$\bar{\nu}_j$	[-]	Net stoichiometric coefficient of reaction j
$\tau = \frac{t}{L/v^{\theta}}$	[-]	Time
$\omega = \frac{v}{v^{\theta}}$	[-]	True gas velocity
$\Psi = \frac{(1-\varepsilon) c_{p,s}}{\varepsilon c_{p,g}}$	[-]	Heat capacity of the fixed bed

Lower indices

e	Outside the reactor
Fe	Iron species
i	Gas component
j	Reaction

Upper indices

G	Gas phase
S	Solid phase, fixed bed
θ	Standard value

References

Galvita, V., Sundmacher, K., "Cyclic water gas shift reactor (CWGS) for carbon monoxide removal from hydrogen feed gas for PEM fuel cells", Chem. Eng. J., 134, 168-174 (2007).

Glöckler, B., Kolios, G., Eigenberger, G., "Analysis of a novel reverse-flow reactor concept for autothermal methane steam reforming", Chem. Eng. Sci., 58, 593-601 (2003).

Hacker, V., Faleschini, G., Fuchsa, H., Fankhauser, R., Simader, G., Ghaemi, M. Spreitz, B., Friedrich, K., "Usage of biomass gas for fuel cells by the SIR process", J. Power Sources, 71, 226-230 (1998).

Hacker, V., Fankhauser, R., Faleschini, G., Fuchs, H., Friedrich, K., Muhr, M., Kordesch, K., "Hydrogen production by steam-iron process", J. Power Sources, 86, 531-535 (2000).

Kulkarni, M.S., Dudukovic, M.P., “Periodic operation of asymmetric bidirectional fixed-bed reactors with temperature limitations”, Ind. Eng. Chem. Res., 37(3), 770-781 (1998).

Lynum, S., Hox, K., Hugdahl, J., “Method and device for the pyrolytic decomposition of hydrocarbons”, Patent US 5997837 (1999).

Malek, A., Farooq, S., “Hydrogen purification from refinery fuel gas by pressure swing adsorption”, AIChE Journal 44, 9, 1985-1992 (1998).

Matros, Y.S., Bunimovich, G.A., Noskov, A.S., “The decontamination of gases by unsteady-state catalytic method. Theory and Practice”, Catalysis Today, 17, 261-274 (1993).

Matros, Y.S., Delmon, B., Yates, J.T. (Eds.), “Catalytic Processes under Unsteady-State Conditions”, in: “Studies in Surface Science and Catalysis” , 43, Elsevier, (1989).

Messerschmitt, “Verfahren zur Erzeugung von Wasserstoff durch abwechselnde Oxidation and Reduktion von Eisen in von außen beheizten, in den Heizräumen angeordneten Zersetzern”, German Patent DE 266863 (1911).

Sircar, S., Golden, T.C., “Purification of hydrogen by pressure swing adsorption”, Sep. Sci. & Tech. 35, 5, 667-687 (2000).